Alma Mater Studiorum - Università di Bologna

Dipartimento di Fisica e Astronomia
Corso di Laurea in Astronomia

QUASI-NORMAL MODES AND ASTROPHYSICAL APPLICATIONS

Tesi di laurea

Presentata da:
Sebastien Sonet

Relatore:
Chiar.ma Prof.ssa Marcella Brusa

Co-Relatore:
Chiar.mo Prof. Karl Landsteiner

Anno Accademico 2023-2024

Introduzione

Nella prima parte ci occupiamo del calcolo dei modi quasi-normali (Quasi-normal modes: "QNMs") per un campo scalare in uno spaziotempo bidimensionale, utilizzando tecniche computazionali. Per i calcoli ci affidiamo a SageMath e impieghiamo metodi pseudospettrali basati su approssimazioni di Chebyshev, garantendo così elevata precisione. Partendo dalla metrica dello spaziotempo, ricaviamo l'equazione del moto per il campo scalare, applichiamo le condizioni al contorno appropriate e trasformiamo l'equazione differenziale di secondo ordine in un sistema del primo ordine. Le frequenze dei QNMs vengono infine ottenute calcolando gli autovalori della matrice risultante.

Nella seconda parte, mostriamo come i QNMs possano essere rilevati attraverso interferometri per onde gravitazionali. Presentiamo la prima rilevazione della fusione di due buchi neri, insieme a diverse altre osservazioni di rilievo.

Contents

Chapter 1

Quasi-normal modes

1.1 Metric

We consider a two-dimensional metric:

$$ds^2 = -(1-x^2)dt^2 + \frac{1}{1-x^2}dx^2, \tag{1.1}$$

It exhibits the same properties of time dilation and spatial expansion as those of the Schwarzschild four-dimensional metric, the metric of a black-hole:

$$ds^2 = -\left(1 - \frac{2GM}{r}\right)dt^2 + \left(1 - \frac{2GM}{r}\right)^{-1} dr^2 + r^2\,d\theta^2 + r^2 \sin^2\theta\,d\phi^2, \tag{1.2}$$

yet (1.1) is notably simpler.
This metric was chosen due to its mathematical simplicity while still capturing essential characteristics of black hole physics, particularly in relation to Quasi-Normal Modes (QNMs).

The temporal component of this metric indicates that the time dilation factor depends on the spatial coordinate x, and it reduces to zero as x→±1. Conversely, the spatial component shows that the spatial scaling factor diverges as x→±1, suggesting the presence of apparent horizons at these points. Within the interval $-1 < x < 1$, the metric behaves as if it is inside a black hole, whereas outside this interval ($x < -1$ or $x > 1$), it mimics the region outside a black hole. Thus, despite its simplicity, this metric effectively models the key features of black hole spacetime and provides insight into the behavior of QNMs.

1.2 consistency of the chosen metric

We want to confirm that this metric is a solution to Einstein's equations and that it has the same physical proprieties of the Schwarzschild's metric.
We begin with an important Tensor in General relativity, the **Riemann Tensor** $R^{\rho}_{\sigma\mu\nu}$, whose components are:

$$R^{\rho}_{\sigma\mu\nu} = \partial_{\mu}\Gamma^{\rho}_{\nu\sigma} - \partial_{\nu}\Gamma^{\rho}_{\mu\sigma} + \Gamma^{\rho}_{\mu\lambda}\Gamma^{\lambda}_{\nu\sigma} - \Gamma^{\rho}_{\nu\lambda}\Gamma^{\lambda}_{\mu\sigma}, \tag{1.3}$$

we use Einstein summation convention.

$\Gamma^{\rho}_{\mu\nu}$ are the **Christoffel symbols**:

$$\Gamma^{\rho}_{\mu\nu} = \frac{1}{2}g^{\rho\lambda}\left(\partial_{\mu}g_{\nu\lambda} + \partial_{\nu}g_{\mu\lambda} - \partial_{\lambda}g_{\mu\nu}\right), \tag{1.4}$$

with $g_{\mu\nu}$ being the **metric tensor**, and $g^{\mu\nu}$ its inverse:

$$g_{\mu\nu} = \begin{pmatrix} -(1-x^2) & 0 \\ 0 & \frac{1}{1-x^2} \end{pmatrix}, \tag{1.5}$$

$$g^{\mu\nu} = \begin{pmatrix} -\frac{1}{1-x^2} & 0 \\ 0 & 1-x^2 \end{pmatrix}. \tag{1.6}$$

We should calculate the $D^3 = 8$ different symbols, but in (1.4) we see that $\Gamma^{\rho}_{\mu\nu} = \Gamma^{\rho}_{\nu\mu}$, so only 6 are independent.
For example:

$$\Gamma^{1}_{00} = \frac{1}{2}g^{1\lambda}\left(\partial_0 g_{0\lambda} + \partial_0 g_{0\lambda} - \partial_{\lambda}g_{00}\right) \tag{1.7}$$

$$= \frac{1}{2}g^{10}\left(\partial_0 g_{00} + \partial_0 g_{00} - \partial_0 g_{00}\right) + \frac{1}{2}g^{11}\left(\partial_0 g_{01} + \partial_0 g_{00} - \partial_1 g_{00}\right),$$

the metric is diagonal, so $g^{10} = g_{01} = 0$:

$$\Gamma^{1}_{00} = \frac{1}{2}(1-x^2)\left(-\partial_t(1-x^2) + \partial_x(1-x^2)\right)$$

$$= \frac{1}{2}(1-x^2)\left(\frac{\partial}{\partial x}(1-x^2)\right) = -x(1-x^2)$$

In the same way we calculate the others:

$$\Gamma^{0}_{00} = 0 \qquad \Gamma^{0}_{01} = \Gamma^{0}_{10} = -\frac{x}{1-x^2} \qquad \Gamma^{0}_{11} = 0$$

$$\Gamma^{1}_{00} = -x(1-x^2) \qquad \Gamma^{1}_{01} = \Gamma^{1}_{10} = 0 \qquad \Gamma^{1}_{11} = \frac{x}{1-x^2}$$

The Riemann Tensor has $D^4 = 16$ components, but it can be observed that, due to various symmetry and anti-symmetry properties over the exchange of symbol pairs, in D=2 there are 4 non-zero components, but only 1 independent:

$$R^1_{001} \qquad R^1_{010} = -R^1_{001}$$

$$R^0_{110} = \tfrac{g^{00}}{g^{11}} R^1_{001} \qquad R^0_{101} = -\tfrac{g^{00}}{g^{11}} R^1_{001}$$

By (1.3) we calculate R^1_{001}:

$$R^1_{001} = \partial_0 \Gamma^1_{10} - \partial_1 \Gamma^1_{00} + \Gamma^1_{0\lambda}\Gamma^\lambda_{10} - \Gamma^1_{1\lambda}\Gamma^\lambda_{00} = 1 - x^2 \tag{1.8}$$

In this way the Reimann tensor has components:

$$R^1_{001} = 1 - x^2 \qquad R^1_{010} = -(1 - x^2)$$

$$R^0_{110} = -\tfrac{1}{1-x^2} \qquad R^0_{101} = \tfrac{1}{1-x^2},$$

all the others are 0.

We can use the Riemann tensor to obtain the **Ricci tensor**:

$$R_{\mu\nu} = R^\lambda_{\mu\lambda\nu}, \tag{1.9}$$

with simple calculations we have its four components:

$$R_{00} = -(1 - x^2) \qquad R_{01} = 0$$

$$R_{10} = 0 \qquad R_{11} = \tfrac{1}{1-x^2}$$

We calculate the **Ricci scalar**:

$$R = R^\lambda_\lambda \tag{1.10}$$

$$= R^0_0 + R^1_1 = g^{0\lambda} R_{\lambda 0} + g^{1\lambda} R_{\lambda 1} = \frac{1}{1-x^2}(1-x^2) + (1-x^2)\frac{1}{1-x^2} = 2.$$

We can now read the **Einstein's equation**:

$$R_{\mu\nu} - \frac{1}{2} R g_{\mu\nu} = \frac{8\pi G}{c^4} T_{\mu\nu}, \tag{1.11}$$

G is the gravitational constant

c is the speed of light

$T_{\mu\nu}$ is the stress-energy tensor, which describes the distribution of energy density and energy flux throughout spacetime; it contains information about the matter and energy content of the system.

We insert the quantities that we know:

$$\begin{pmatrix} -(1-x^2) & 0 \\ 0 & \frac{1}{1-x^2} \end{pmatrix} - \frac{1}{2} \cdot 2 \begin{pmatrix} -(1-x^2) & 0 \\ 0 & \frac{1}{1-x^2} \end{pmatrix} = \frac{8\pi G}{c^4} T_{\mu\nu}, \tag{1.12}$$

$$\begin{pmatrix} 0 & 0 \\ 0 & 0 \end{pmatrix} = \frac{8\pi G}{c^4} T_{\mu\nu}, \tag{1.13}$$

We have demonstrated that the metric (1.1) is a solution to Einstein's equation only if $T_{\mu\nu} = 0$.

The Schwarzschild's metric is derived by imposing the following conditions:

- The Einstein's equation valid, with $T_{\mu\nu} = 0$ because we want a space-time where there is no matter o energy density
- a spherical symmetric problem

So we've shown that the metric (1.1) is a solution to Einstein's equation in a two-dimensional space-time where we have the same physical proprieties as (1.2). This allows us to say that (1.1) is a metric of a hypothetical black hole in two dimensions, considered within Einstein's theory.

1.3 Derivation of the equation of motion

The Lagrangian is:

$$\mathcal{L} = T - V \tag{1.14}$$

We consider a scalar field Φ:

$$\Phi : \mathbb{R}^{N-1} \times \mathbb{R} \to \mathbb{C}, \quad (\vec{x}, t) = \vec{q} \mapsto \Phi(\vec{x}, t) = \Phi(\vec{q}), \tag{1.15}$$

in a certain N dimensional metric, the simplest form for it to be a scalar, that is to say a rank (0,0) tensor, is the form:

$$\mathcal{L} = -\frac{1}{2} g^{\mu\nu} \partial_\mu \Phi \, \partial_\nu \Phi - \frac{1}{2} m^2 \Phi^2, \tag{1.16}$$

it can be proved that this transform like a tensor. From this Lagrangian we construct the action S:

$$S = \int \sqrt{-g} \left(-\frac{1}{2} g^{\mu\nu} \partial_\mu \Phi \, \partial_\nu \Phi - \frac{1}{2} m^2 \Phi^2 \right) d^N q, \tag{1.17}$$

where g is the determinant of $g_{\mu\nu}$, $\sqrt{-g}$ is a factor of normalisation inserted to ensure that the action is still a scalar.

The equation of motion, that govern how $\Phi(\vec{q})$ behaves is:

$$\frac{\delta S}{\delta \Phi} = 0, \tag{1.18}$$

(1.18) can happen only if:

$$S[\Phi + \delta\Phi] - S[\delta\Phi] = 0, \tag{1.19}$$

which means:

$$\int \sqrt{-g} \left(-\frac{1}{2} g^{\mu\nu} \partial_\mu (\Phi + \delta\Phi) \, \partial_\nu (\Phi + \delta\Phi) - \frac{1}{2} m^2 (\Phi + \delta\Phi)^2 \right) d^N q$$
$$- \int \sqrt{-g} \left(-\frac{1}{2} g^{\mu\nu} \partial_\mu \Phi \, \partial_\nu \Phi - \frac{1}{2} m^2 \Phi^2 \right) d^N q = 0$$

Whit some step, not including the terms of second order in $\delta\Phi$ we get:

$$\int \left(\sqrt{-g} \left(-g^{\mu\nu} \partial_\mu \Phi \partial_\nu \delta\Phi \right) - \sqrt{-g} \left(m^2 \Phi \delta\Phi \right) \right) d^N q = 0 \tag{1.20}$$

We integrate by part the first addend, and let $\delta\Phi = 0$ at the limits of the domain:

$$\int \delta\Phi \left(\partial\mu \left(\sqrt{-g} g^{\mu\nu} \partial_\nu \Phi \right) - \sqrt{-g} \left(m^2 \Phi \right) \right) d^N q = 0 \tag{1.21}$$

For an arbitrary $\delta\Phi$ (1.21) is true only if:

$$\frac{1}{\sqrt{-g}} \partial_\mu \left(\sqrt{-g} \, g^{\mu\nu} \partial_\nu \Phi \right) - m^2 \Phi = 0 \tag{1.22}$$

(1.22) is the Klein-Gordon equation, it describes how a scalar function Φ behaves in a N-dimensional spacetime with a certain metric $g_{\mu\nu}$.
So given the metric $g_{\mu\nu}$, an arbitrary scalar function Φ must satisfy (1.22).

1.4 Equation of motion in our metric

In our particular case, we see that $\sqrt{-g} = 1$ and that the metric is diagonal, so:

$$\frac{1}{\sqrt{-g}}\partial_\mu\left(\sqrt{-g}\,g^{\mu\nu}\partial_\nu\Phi\right) = \partial_0\left(g^{00}\partial_0\Phi\right) + \partial_1\left(g^{11}\partial_1\Phi\right) = \tag{1.23}$$

$$= \partial_t\left(\frac{-1}{1-x^2}\partial_t\Phi\right) + \partial_x\left((1-x^2)\partial_x\Phi\right)$$

$$= \frac{-1}{1-x^2}\partial_t^2\Phi + \partial_x\left((1-x^2)\partial_x\Phi\right), \tag{1.24}$$

With m=1 the Klein-Gordon equation becomes:

$$-\frac{1}{1-x^2}\frac{\partial^2\Phi}{\partial t^2} + \frac{\partial}{\partial x}\left((1-x^2)\frac{\partial}{\partial x}\Phi\right) - \Phi = 0. \tag{1.25}$$

This is the equation we need to solve to determine the behaviour of the scalar field in this spacetime.

We propose a specific form for the solution, namely:

$$\Phi(x,t) = \Phi_t(t)\eta(x) \tag{1.26}$$

Here we've done the separation of variables.
We plot this in the equation, then divide by the function:

$$-\frac{1}{\Phi_t}\frac{1}{1-x^2}\frac{\partial^2\Phi_t}{\partial t^2} + \frac{1}{\eta}\frac{\partial}{\partial x}\left((1-x^2)\frac{\partial}{\partial x}\eta\right) - 1 = 0 \tag{1.27}$$

We moltiply by $(1-x^2)$ and note that there are two separeted part of the equation, one with only the t variable and the other with the single x variable. The only way that it is still valid for all x and t is that the two parts are constants in the general complex domain:

$$\underbrace{-\frac{1}{\Phi_t(t)}\frac{\partial^2\Phi_t(t)}{\partial t^2}}_{\text{constant}} + \underbrace{\frac{1-x^2}{\eta(x)}\frac{\partial}{\partial x}\left((1-x^2)\frac{\partial}{\partial x}\eta(x)\right) - (1-x^2)}_{\text{constant}} = 0 \tag{1.28}$$

The first part assure that Φ_t has to be eigen-function of $\frac{\partial^2\Phi_t}{\partial t^2} \propto \Phi_t$, the generic form is $\Phi_t = e^{-i\omega t}$, with $\omega \in \mathbb{C}$.
We can now find, with a few steps:

$$\frac{\omega^2\eta(x)}{(x^2-1)^2} + \frac{2x\frac{\partial}{\partial x}\eta(x)}{(x^2-1)} + \frac{\eta(x)}{(x^2-1)} + \frac{\partial^2}{\partial x^2}\eta(x) = 0 \tag{1.29}$$

We eliminated the time-component of the equation and find a differential equation in only one variable.

1.5 Boundary conditions

The boundary conditions for the problem are implicitly incorporated into the proposed solution of the form:

$$\eta(x) = (1-x)^{-i\omega/2}(1+x)^{-i\omega/2}\zeta(x) \tag{1.30}$$

we are effectively specifying boundary conditions that restrict the behavior of the scalar field.
The boundary conditions implicitly enforce that the scalar field behaves as a propagating wave with a well-defined direction of propagation. Specifically, we choose only the waves that propagate from x=0 towards the event horizon (x=±1). We consider only the waves that enter the event horizon(in-coming waves), not those that exit(out-going waves).
If we start to implement this form in the equation, we would calculate the derivatives of η:

$$\frac{\partial}{\partial x}\eta = i\frac{\omega}{2}(1-x)^{-i\frac{\omega}{2}-1}(1+x)^{-i\frac{\omega}{2}}\zeta - i\frac{\omega}{2}(1-x)^{-i\frac{\omega}{2}}(1+x)^{-i\frac{\omega}{2}-1}\zeta + (1-x)^{-i\frac{\omega}{2}}(1+x)^{-i\frac{\omega}{2}}\frac{\partial}{\partial x}\zeta \tag{1.31}$$

The equation would start to be long when we see the second derivative, so, instead we can do the calculation with Sagemath, it simplifies the problem in the final form:

$$\omega^2\zeta(x) + (2ix\frac{\partial}{\partial x}\zeta(x) + i\zeta(x))\omega - 2x\frac{\partial}{\partial x}\zeta(x) - (x^2-1)\frac{\partial^2}{\partial x^2}\zeta(x) - \zeta(x) = 0 \tag{1.32}$$

1.6 Eigen value equation and pseudospectral methods

Now we want to construct an eigenvalue equation in the form:

$$L\hat{\Phi} = \lambda\hat{\Phi}, \tag{1.33}$$

where L is a differential operator in x which is not dependent on ω, $\hat{\Phi}$ is the eigen vector which is function of ζ, and λ are the eigen-values which are function of ω.
To do this, we say:

$$\begin{pmatrix} 0 & 1 \\ L_1 & L_2 \end{pmatrix}\begin{pmatrix} \zeta \\ \phi \end{pmatrix} = -i\omega\begin{pmatrix} \zeta \\ \phi \end{pmatrix} \tag{1.34}$$

where:

$$L_1 = (1-x^2)\frac{\partial^2}{\partial x^2} - 2x\frac{\partial}{\partial x} - 1, L_2 = -2x\frac{\partial}{\partial x} - 1$$

$$\hat{\Phi} = \begin{pmatrix} \zeta \\ \phi \end{pmatrix}, \lambda = -i\omega$$

These definitions satisfies the previous requests with the first equation being a definition: $\phi = -i\omega\zeta$; and the second the equation of motion.

We address the solution of an eigenvalue problem using pseudospectral methods. Specifically, we employ Chebyshev approximations to find the eigenvalues of a given differential operator. The methodology is inspired by the techniques outlined in Trefethen's book "Spectral Methods in MATLAB". The Chebyshev grid points x_j for $j = 0, 1, \ldots, N$ are given by:

$$x_j = \cos\left(\frac{j\pi}{N}\right), \tag{1.35}$$

with N initial input parameter.
The derivatives on the Chebyshev grid are matrices implemented in Sagemath by default.
The program calculates the eigen-values of the matrix L and we multiple by i to obtain ω.
Finally we have a L matrix 2N x 2N and eigen vector of leght 2N.
With N=15, we get our final result, the ω:

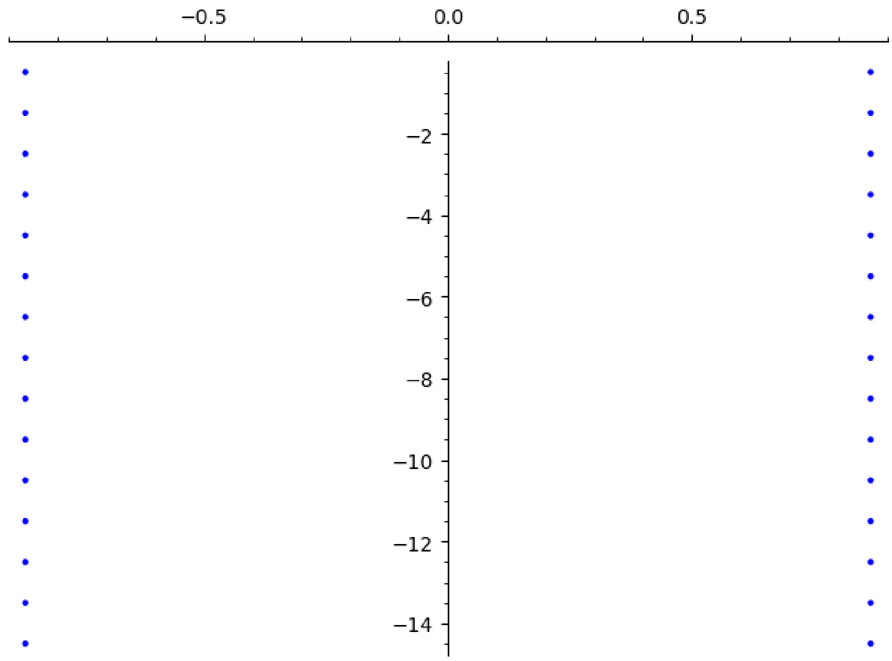

Figure 1.1: orizontal axis: real part, vertical axis: imaginary part of ω

There is an important structure: the real part is only +1 or -1, the imaginary part is always negative and between two eigen-value there is always the same distance

1.7 Interpretations of the result

If $\omega = \Omega + \mathrm{i}\Gamma$, with $\Omega, \Gamma \in \mathbb{R}$ we see that our function is:

$$\Phi(x,t) = e^{-i\Omega t} e^{\Gamma t} \eta(x)$$

There are only $\Gamma < 0$, it means that as the time passes the whole Φ decay exponentially.
It can be seen that, if the boundary conditions were in-coming waves:

$$\eta(x) = (1-x)^{+i\omega/2}(1+x)^{+i\omega/2}\zeta(x), \tag{1.36}$$

the Γ would be always positive, which would bring the functions to grow exponentially in time, this is something non-physical, meaning that we can't have outgoing waves.
If $\eta(x) = \chi(x) + i\Theta(x)$, with χ,Θ functions of $\mathbb{R}$, knowing:

$$e^{ix} = \cos(x) + i\sin(x), \tag{1.37}$$

we separate the real part from the imaginary one and we get:

$$\Phi(x,t) = e^{\Gamma t}(\cos(\Omega t)\chi(x) + \sin(\Omega t)\Theta(x)) + ie^{\Gamma t}(\cos(\Omega t)\Theta(x) - \sin(\Omega t)\chi(x)) \tag{1.38}$$

$\forall$ x in $\mathbf{R}$ we can compute how $\Phi(x,t)$ behaves as time passes; in particular, we assume that at a certain x: $\chi(x) = C\Theta(x)$, with C $\in \mathbf{R}$.
By doing it, we compute the real and the imaginary part of $\Phi(x,t)$, at a fixed x :

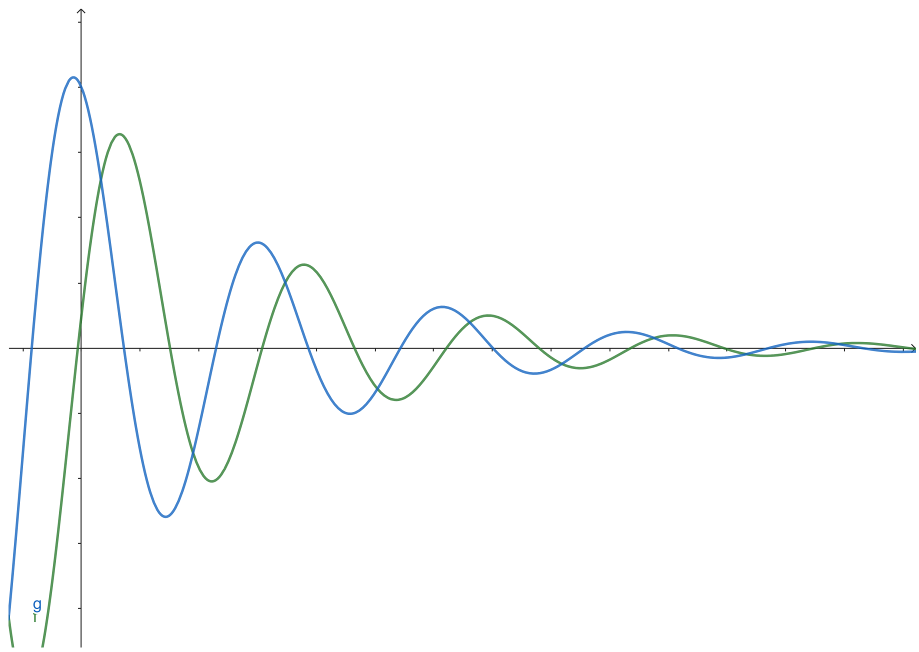

Figure 1.2: x-axis is time, y-axis is intensity; the green function is the real part of Φ the blue one is the imaginary part of Φ

The result is that the functions are exponentially damped sinusoids.
For different ω we observe:
-) Oscillations with the same frequencies, which are determined by Ω, and can only be ± 1;
-) Different rates of decay for functions, governed by varying values of Γ, which determine how quickly they decay.
Given this metric, if we know a scalar function at a fixed position in a specific time t this is how it behaves when time passes.
We calculated a simplified version of a Black-hole, that it is in a 4D metric instead, but they give the same type of ω.

Chapter 2

Astrophysical applications

Quasi-normal modes of black holes are solutions of Einstein's equations when we apply perturbation theory to a Schwarzschild metric background. A simplified approach to obtain QNMs is to find solutions to the equation of motion for a scalar field in a fixed Schwarzschild metric, like we did. So it's like studying a specific scalar function correlated with black holes: the intensity of gravitational waves(GW).

2.1 Gravitational waves

Gravitational wave detection is the observation of ripples in spacetime caused by massive cosmic events, such as merging black holes or neutron stars. These waves were first predicted by Einstein's theory of General Relativity in 1916. However, they were only directly detected in 2015 by the LIGO (Laser Interferometer Gravitational-Wave Observatory) collaboration.
Detectors like LIGO (located in Hanford, Washington, and Livingston, Louisiana) and Virgo (near Pisa, Italy) use laser interferometry to detect gravitational waves. These facilities have long L-shaped arms, each several kilometers long, through which laser beams travel. When a gravitational wave passes, it slightly distorts spacetime, causing one arm to lengthen and the other to shorten. This minuscule change in distance alters the laser beam's interference pattern, allowing scientists to detect the wave.
In 1960s-1970s were developed initial concepts and prototypes, in the 1990s LIGO and Virgo projects were initiated. In 2015 LIGO made the first detection of gravitational waves from a binary black hole merger. In 2017 Both LIGO and Virgo detected waves from a neutron star merger, also observed by electromagnetic telescopes. Since that, we observed 96 events. These observatories have opened a new era of astronomy, allowing us to observe the universe through gravitational waves, providing insights into previously unseen cosmic phenomena.
We studied what happen in a metric of a single black hole, this means that our subject is gravitational waves from a metric of a single black hole. The only time we can observe QNMs is shortly after the merger of two big astronomical objects, as the metric is governed by the single, final object and the signal's intensity is extremely high, which is necessary due to detection limitations.

2.2 First detected event

On September 14, 2015 at 09:50:45 UTC, the two detectors of the Laser Interferometer Gravitational-Wave Observatory simultaneously observed a transient gravitational-wave signal. In only 0.2 s the signal sweeps upwards in frequency from 35 to 250 Hz, this GW derives from the orbiting of the black holes, particularly the signal frequency is the double of the orbital frequency. The maximal intensity of the GW is when they merge, this peak of gravitational-wave strain is 1.0×10^{-21}; it means that the gravitational wave causes a change in the distances between points in space by one part in 10^{21}.

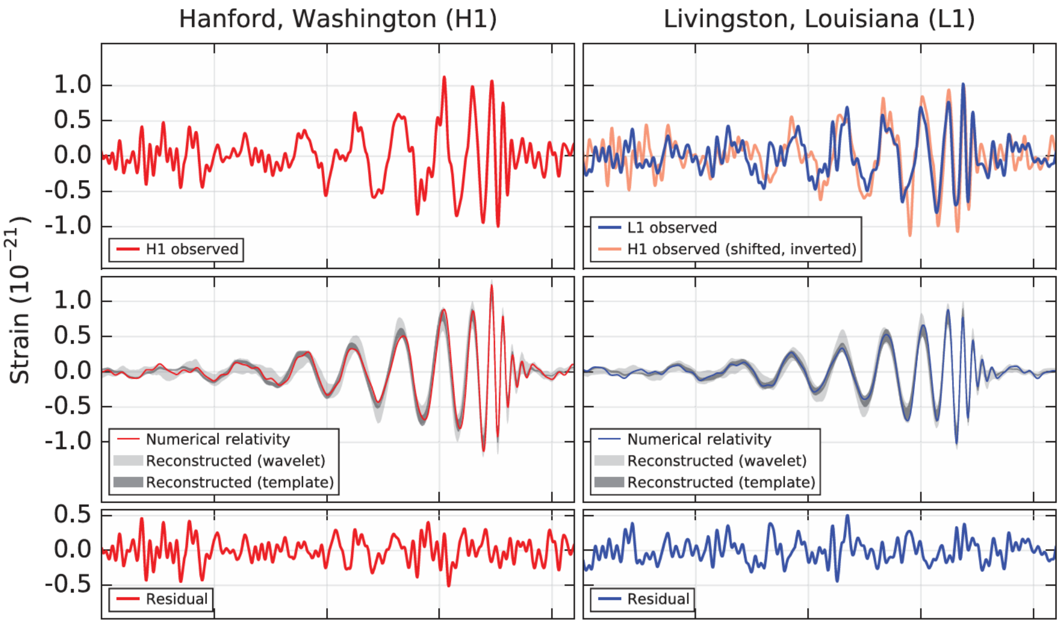

Figure 2.1: The gravitational-wave event GW150914 observed by the LIGO Hanford (H1, left column panels) and Livingston (L1, right column panels) detectors. Top row, left: H1 strain. Top row, right: L1 strain. Second row: Gravitational-wave strain projected onto each detector in the 35–350 Hz band. Solid lines show a numerical relativity waveform. Shaded areas show 90 % credible regions for two independent waveform reconstructions. One (dark gray) models the signal using binary black hole template waveforms. The other (light gray) does not use an astrophysical model, but instead calculates the strain signal as a linear combination of sine-Gaussian wavelets. Third row: Residuals after subtracting the filtered numerical relativity waveform from the filtered detector time series

It matches the waveform predicted by general relativity for the inspiral and merger of a pair of black holes and the ringdown of the resulting single black hole. The signal was observed with a matched-filter signal-to-noise ratio of 24 and a false alarm rate estimated to be less than 1 event per 203,000 years, equivalent to a significance greater than 5.1σ. The source lies at a luminosity distance of 410^{+160}_{-180} Mpc corresponding to a redshift $z = 0.09^{+0.03}_{-0.04}$. In the source frame, the initial black hole masses are $36^{+5}_{-4}\,M_\odot$ and $29^{+4}_{-4}\,M_\odot$, and the final black hole mass is $62^{+4}_{-4}\,M_\odot$, with $3.0^{+0.5}_{-0.5}\,M_\odot c^2$ radiated in gravitational waves. These observations demonstrate the existence of binary stellar-mass black hole systems. This is the first direct detection of gravitational waves and the first observation of a binary black hole merger. In this case they reconstruct the relative velocity over time: it reaches 0.6 c; and the separations between the black holes.

They observe quasi-normal modes (QNMs) after the merger, a process known as **ring-down**. As expected, the frequency of the signal remains consistent across the range of QNMs, from the moment of the merger until the signal becomes indistinguishable from the noise, which occurs within a fraction of a second. During this process, the signal decays over time.

These observations provide two pieces of information that combine into a single complex number, denoted as ω. In reality, the Schwarzschild metric gives rise to QNMs with a range of ω values directly associated with the parameters of spherical harmonics. This is because the Schwarzschild metric includes an angular component, which we have not considered in our simplified case.

What happens is that there are superposition of ω values, weighted by the significance of each spherical harmonic in the overall scalar function. The result is a final complex frequency described by a superposition of ω values that match the structure we found, with specific signal frequencies and decay times observable in practice.

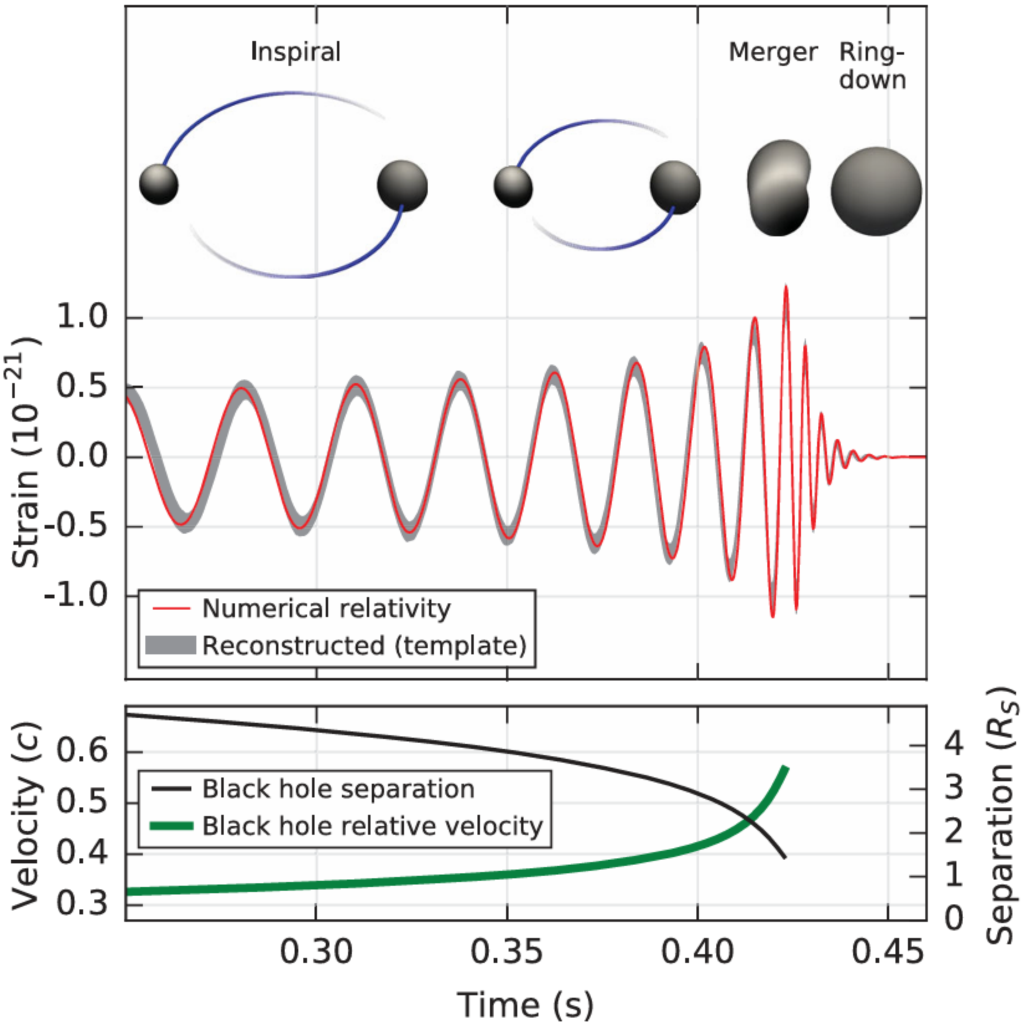

Figure 2.2: Top: Estimated gravitational-wave strain amplitude from GW150914 projected onto H1. This shows the full bandwidth of the waveforms, without the filtering used for Fig. 2.1. The inset images show numerical relativity models of the black hole horizons as the black holes coalesce. Bottom: The effective black hole separation in units of Schwarzschild radii ($R_S = \frac{2GM}{c^2}$) and the effective relative velocity given by the parameter $\frac{v}{c} = (\frac{GMf\pi}{c^3})^{\frac{1}{3}}$, where f is the gravitational-wave frequency calculated with numerical relativity and M is the total mass

2.3 Other detected events

Over the following years they've detected the merging of 96 Astrophysical objects: Binary black holes (BBH), Neutron stars-Black hole (NSBH) and Binary Neutron stars(BNS).
Recent gravitational wave events have provided crucial tests for Einstein's theory of General Relativity, confirming its predictions with remarkable precision. Observations of black hole and neutron star mergers have matched the theory's expectations,

reinforcing General Relativity as the most accurate framework we have for understanding gravity, even under extreme conditions.
One of the confirmations of General Relativity has been the detection of Quasi-Normal Modes (QNMs) in gravitational wave signals, these oscillations, observed during the "ringdown" phase, match theoretical predictions.
Numerous studies have explored Quasi-Normal Modes (QNMs) by analyzing the superposition of various frequencies associated with different eigenvalues of spherical harmonics. However, one study specifically focused on the fundamental oscillation mode for certain events and found that its frequency is consistent with observations. In this analysis, they focus solely on the fundamental mode, as the higher modes are considered irrelevant for this investigation. Specifically, they found no significant evidence for the presence of higher modes. However, non-stationary noise introduces a degree of uncertainty, meaning that while the higher modes are disregarded here, their actual relevance remains inconclusive due to the noise affecting the signal analysis. They've compared for five events the predicted fundamental mode l=$|m|$=2 and n=0 (inspiral–merger–ringdown(IMR)) with a single damped sinusoid (DS) fitted from the data.

Event	**Redshifted frequency [Hz]**		**Redshifted damping time [ms]**	
	IMR	**DS**	**IMR**	**DS**
GW191109_010717	120^{+8}_{-6}	104^{+10}_{-6}	$7.8^{+2.5}_{-1.0}$	$14.6^{+6.1}_{-4.0}$
GW191222_033537	147^{+13}_{-14}	157^{+772}_{-63}	$6.9^{+1.1}_{-0.8}$	$15.3^{+30.4}_{-12.1}$
GW200129_065458	251^{+9}_{-11}	217^{+27}_{-51}	$4.5^{+0.5}_{-0.4}$	$2.8^{+2.4}_{-1.2}$
GW200224_222234	197^{+9}_{-8}	195^{+11}_{-13}	$5.6^{+0.6}_{-0.5}$	$7.3^{+6.3}_{-3.3}$
GW200311_115853	236^{+10}_{-13}	320^{+630}_{-246}	$4.4^{+0.5}_{-0.4}$	$21.7^{+25.3}_{-19.6}$

Table 2.1: The median and 90 % credible regions of the redshifted frequency and damping time from a single damped-sinusoid(DS) analysis, compared to the IMR predictions for the fundamental mode(220)

Theory and observations generally agree, though not perfectly, due to the following considerations:

- The theory considers superpositions of modes, while only the fundamental mode is accounted for here
- The frequency and damping time (IMR) depend directly on the final mass and spin of the black hole, so errors in these parameters can propagate
- There is also the error introduced by the detector

With these considerations in mind, the results are considered quite accurate. More precise predictions that account for superpositions of ω have been made, but we will not report them here. We hope that future advancements in detector technology will allow for clearer observations of the final stage of the ring-down and enable the detection of quasi-normal modes with greater precision.

Acknowledgments

I would like to express my gratitude to **Prof. Karl Landsteiner**, for his guidance through this work, especially I thank his ability to give me inputs for finding results by myself while always helping me if I couldn't find them.

Bibliography

LIGO, Virgo and KAGRA Collaboration, 2022, *Tests of General Relativity with GWTC-3*, Physical review letters

LIGO and Virgo Collaboration, 2016, *Observation of Gravitational Waves from a Binary Black Hole Merger*, Physical review letters

Trefethen L. N., 2000, *Spectral Methods in Matlab*, SIAM